Applied Catalysis A: General 391 (2011) 360–366

Applied Catalysis A: General

journal homepage: www.elsevier.com/locate/apcata

Production of hydrogen from dimethyl ether on supported Au catalysts

A. Gazsi, I. Ugrai, F. Solymosi*

Reaction Kinetics Research Group, Chemical Research Centre of the Hungarian Academy of Sciences, Department of Physical Chemistry and Materials Science, University of Szeged, P.O. Box 168, H-6701 Szeged, Hungary

ARTICLE INFO

Article history:
Received 17 February 2010
Received in revised form 31 March 2010
Accepted 26 April 2010
Available online 5 May 2010

Keywords:
IR spectra of adsorbed dimethyl ether
Decomposition of dimethyl ether
Reforming of dimethyl ether
Hydrogen production
Au catalyst
CeO_2 support

ABSTRACT

The adsorption and reactions of dimethyl ether (DME) were investigated on Au nanoparticles supported by various oxides and carbon Norit. Infrared spectroscopic and temperature programmed desorption studies revealed that DME adsorbs readily on most oxidic supports. A limited dissociation of DME to methoxy species was established on Au particles by IR spectroscopy. As regards the formation of hydrogen, Au/CeO_2 is the most effective catalyst. On Au/Al_2O_3 catalyst the main process was the formation of methanol with a very small amount of hydrogen. Deposition of Au on CeO_2–Al_2O_3 mixed oxide resulted in a very active catalyst for H_2 production. The yield for H_2 in the reforming of DME approached the value of 73% at 723–773 K. This feature was explained by the hydrolysis of DME to methanol on alumina, and the fast decomposition of methanol at the Au/CeO_2 interface. Adding potassium promoter to Au/CeO_2–Al_2O_3 catalyst further enhanced the production of hydrogen as indicated by the increase of the yield to ~87%. No deactivation of the catalyst was experienced at 773 K for the measured time, ~10 h.

1. Introduction

A great effort is being made nowadays to develop catalytic processes for the generation of hydrogen [1,2]. Ethanol and methanol are the most generally used materials. However, an increasing interest can be observed in the use of dimethyl ether (DME), which also contains a large amount of hydrogen, and appears to be a suitable compound for the source of hydrogen. DME possesses several advantageous properties and applications. It is considered as an alternative fuel replacing diesel, as its burning produces much less pollutant [3–5]. In the last decade, several catalytic reactions of DME including its combustion, dehydrogenation, hydrolysis, selective oxidation, transformation to hydrocarbons [6] and even aromatization have been studied [7]. As it is non-toxic, thus more preferable compared to methanol to use it as a hydrogen carrier for fuel cells. The decomposition and reforming of DME to hydrogen were also investigated on various catalysts [8–18]. The more effective ones are the Pt metals, which are able to rupture the C–C bond. An alternative solution for the use of cheaper but less active catalyst is to apply a composite catalyst [16,18]. In this way we were able to enhance the catalytic activity of Mo_2C prepared on carbon Norit in the production of H_2 from DME [16].

In the present work we report the adsorption, decomposition and reforming of DME on supported Au catalysts. Following the pioneering work of Haruta et al. [19] the supported Au nanoparticles exhibited a surprisingly high activity in many reactions [20]. Recently it was demonstrated that the gold metal also catalyses the decomposition and reforming of methanol [21–28] and ethanol [29,30]. The highest yield for hydrogen was obtained on Au/CeO_2 [27,30].

2. Experimental

2.1. Materials and preparation of the catalysts

The following compounds were used as supports. CeO_2 (ALFA AESAR, 50 m^2/g), Al_2O_3 (Degussa P 110 C1, 100 m^2/g), MgO (DAB 6, 170 m^2/g), TiO_2 (Degussa P25, 50 m^2/g), SiO_2 (CAB-O-SiL, 198 m^2/g) and activated carbon Norit (ALFA AESAR, 859 m^2/g). Carbon Norit was purified by treatment with HCl (10%) for 12 h at room temperature. Supported Au catalysts with a gold loading of 1, 2 or 5 wt% were prepared by a deposition–precipitation method. $HAuCl_4$·aq. (p.a., 49% Au, Fluka AG) was first dissolved in triply distilled water. After the pH of the aqueous $HAuCl_4$ solution had been adjusted to 7.5 by the addition of 1 M NaOH solution, a suspension was prepared with the finely powdered oxidic support, and the system was kept at 343 K for 1 h under continuous stirring. The suspension was then aged for 24 h at room temperature, washed repeatedly with distilled water, dried at 353 K and calcined in air at 573 K for 4 h. Similar method was used for the preparation of $Au/CeO_2 + Al_2O_3$. In this case the oxide-mixture (1:1) was impregnated in the $HAuCl_4$·aq. solution. We mark this composite catalyst: "co-impregnated". The fragments of catalyst pellets were oxidized at 673 K and reduced at 673 K for 1 h *in situ*. DME was the product of Gerling Holz +CO (99.9%). Other gases were of commercial purity (Linde).

* Corresponding author. Tel.: +36 62 420 678; fax: +36 62 420 678.
E-mail address: fsolym@chem.u-szeged.hu (F. Solymosi).

0926-860X/$ – see front matter © 2010 Elsevier B.V. All rights reserved.
doi:10.1016/j.apcata.2010.04.054

2.2. Methods

Catalytic reactions were carried out at 1 atm in a quartz tube (8 mm id) that served as a fixed-bed, continuous flow reactor. The flow rate was in general 40 ml/min. The carrier gas was Ar, which was mixed with DME at room temperature. The DME content was approximately 10%. In general, 0.3 g of loosely compressed catalyst sample was used. After reduction of the catalyst, the reactor was flushed with argon for 15 min, and the sample was cooled in an Ar flow to the lowest reaction temperature investigated. After the Ar had been replaced by the reacting gas mixture, the reactor was gradually heated to selected temperatures, at which the gases were analyzed with an HP 5890 gas chromatograph fitted with PORAPAK Q and PORAPAK S packed columns. In the study of the reaction of DME + H_2O mixtures of different compositions, the reactants were introduced into an evaporator with the aid of an infusion pump (MEDICOR ASSISTOR PCI flow rate: 0.3 ml liquid/h): the evaporator was flushed with an Ar flow (36 ml/min). The DME or DME + H_2O mixture containing Ar flow entered the reactor through an externally heated tube in order to avoid condensation. The conversion of DME was calculated by taking into account the amount consumed.

FTIR spectra of adsorbed DME were recorded with a BioRad FTS-155 spectrometer with a wavenumber accuracy of $\pm 4\,cm^{-1}$. The spectrum of the sample after the reduction step was used as background. Thermal desorption measurements (TPD) were carried out in the catalytic reactor. The catalysts were treated with DME/Ar containing 10% DME at ~300 K for 60 min, and then flushed with Ar for 30 min. The TPD was carried out in an Ar flow (20 ml/min) with a ramp at ~2 K/min from ~300 to ~900 K. Desorbing products were analyzed by gas chromatography. Transmission electron microscopy (TEM) images were taken with a Philips CM 20 and a Morgagni 268 D electron microscope at 300 K. Approximately 1 mg of catalyst was placed on a TEM grid. X-ray photoelectron spectroscopy (XPS) images were taken with a Kratos XSAM 800 instrument, using non-monochromatic Al Kα radiation ($h\nu$ = 1486.6 eV) and a 180° hemispherical analyzer at a base pressure of 1×10^{-9} mbar.

3. Results

3.1. Characterization of Au samples

The sizes of Au nanoparticles were measured with an electron microscope. We obtained the following values: 2–3 nm for 1% Au/CeO_2, 3–4 nm for 1% Au/SiO_2, 6–7 nm for 1% Au/TiO_2, 5–6 nm for 1% Au/Norit and 6–7 nm for 1% Au/Al_2O_3. The XP spectra of supported Au catalysts used in the present work have been previously determined [30]. The spectrum for the oxidized 1% Au/CeO_2 sample in the Au $4f_{7/2}$ region showed that most of the Au was in the Au^+ and Au^{3+} states. After reduction of the sample at 673 K, the intensity of the BE for Au^{3+} decreased and that of Au^0 developed. As concerns the XPS region of cerium in the oxidized catalyst, the dominant peaks at 882.6 and 898.4 eV were due to Ce^{4+}. The shoulders at 885.1 and 900.4 eV, however, revealed the presence of Ce^{3+} in the starting material [31–33]. This indicated that the deposition of Au on the CeO_2 leads to a partial reduction of the Ce^{4+} on the surface. These features became more evident after the reduction of the Au/CeO_2 at higher temperatures. After the oxidation of the 2% Au/SiO_2, the peaks in the Au 4f region demonstrated the presence of Au^{3+} and Au^+. The reduction at 673 K increased the intensity of the peak for Au^0, but, similarly as for 1% Au/CeO_2, did not eliminate Au^+ on the surface. On the oxidized Au/Norit sample, there were equal amounts of Au^{3+} and Au^+. After reduction, the BE peak for Au^0 also appeared.

3.2. Infrared spectroscopic measurements

Fig. 1A depicts the IR spectra of DME adsorbed on 1% Au/CeO_2 (T_R = 673 K) at 300 K and heated to different temperatures under continuous degassing. At 300 K, intense absorption bands were observed at 2955, 2894, 2883, and 2838 cm^{-1} and weaker bands or shoulders appeared at ~2999 and 2923 cm^{-1} in the C–H stretching region. In the low-frequency range, absorption bands were identified at 1583, 1519, 1473, 1457, 1375, 1315, 1253, 1158, 1071 and 1035 cm^{-1}. Heating the sample caused the attenuation of all the bands. Virtually identical spectra were measured following the adsorption of DME on pure CeO_2. The difference is that the absorption bands were more stable than those identified on Au/CeO_2. Similar spectral features were found for Au/Al_2O_3 with a very slight deviation in the position of the bands. The results obtained for Au/SiO_2 deserve special mention. The advantage of this sample is that DME adsorbs only weakly and non-dissociatively on silica and it may therefore be expected that the vibration bands observed at higher temperatures are due to the species attached to Au particles. In order to eliminate the absorption bands arising from weakly adsorbed DME, the adsorbed layer was heated to 473 K under continuous degassing. The TPD experiments (see next section) indicated that this treatment is sufficient for the desorption of DME. The IR spectrum for pure SiO_2 contained no detectable spectra features after this treatment. In the presence of 5% Au absorption bands appeared at 2958, 2925, 2912, and 2859 cm^{-1} at 373 K, which attenuated after evacuation of the sample at higher temperature. Nevertheless, most of them can be identified even after heat-treatment at 473–573 K. No peaks were detected below 1300 cm^{-1} due to the low transmittance of SiO_2. IR spectra are displayed in Fig. 1B. Table 1 lists the characteristic vibrations of DME and its possible dissociation products on different solids.

3.3. Thermal desorption measurement

TPD spectra for the various products after the adsorption of DME on the Au catalysts at ~300 K are presented in Fig. 2. For 1% Au/CeO_2 the release of adsorbed DME started slightly above 300 K and peaked at ~370 K. At T_p = 560–580 K, the desorption of H_2 and CH_4 was detected. A very small amount of ethane desorption between 480 and 560 K was also observed (Fig. 2A). Very similar TPD spectra were registered for pure CeO_2. The desorption of DME from 1% Au/Al_2O_3 occurred with a T_p ~ 370 and 510 K. In addition, the release of methanol (T_p = 510 K), H_2, CO and CH_4 with identical peak temperatures, T_p ~ 650 K was also identified (Fig. 2B). When DME was adsorbed on 1% Au/CeO_2–Al_2O_3 catalyst (co-impregnated), the desorption of DME (T_p ~ 380 and 500 K), CO and H_2 (T_p ~ 590 K) was registered (Fig. 2C). From 2% Au/SiO_2 only the desorption of DME (T_p = 350 K) was observed.

3.4. Catalytic studies

Au nanoparticles deposited on SiO_2, MgO and carbon Norit exhibited very slight catalytic effect on the decomposition of DME. Even at 773 K, the conversion was less than 2–3%. Somewhat higher activity was measured on 1% Au/TiO_2 sample, where an appreciable decomposition occurred above 573 K, and the conversion attained 30% at 873 K. The products were CH_4, CH_3OH, H_2, CO and a very small amount of C_2H_6. The yield of H_2 formation, however, was very low, less than 10% even at 773 K. 1% Au/CeO_2 catalyst exhibited a similar catalytic performance than the Au/TiO_2 with the difference that the percentage of H_2 was much higher, 50–60% (Fig. 3A). However due to the low conversion (~20%) the yield of H_2 was less than 15% even at 773 K. A disadvantageous property of Au/CeO_2 is the fast deactivation at 773 K. An increase of Au loading to 5% enhanced only slightly the conversion of DME, which reached the value of

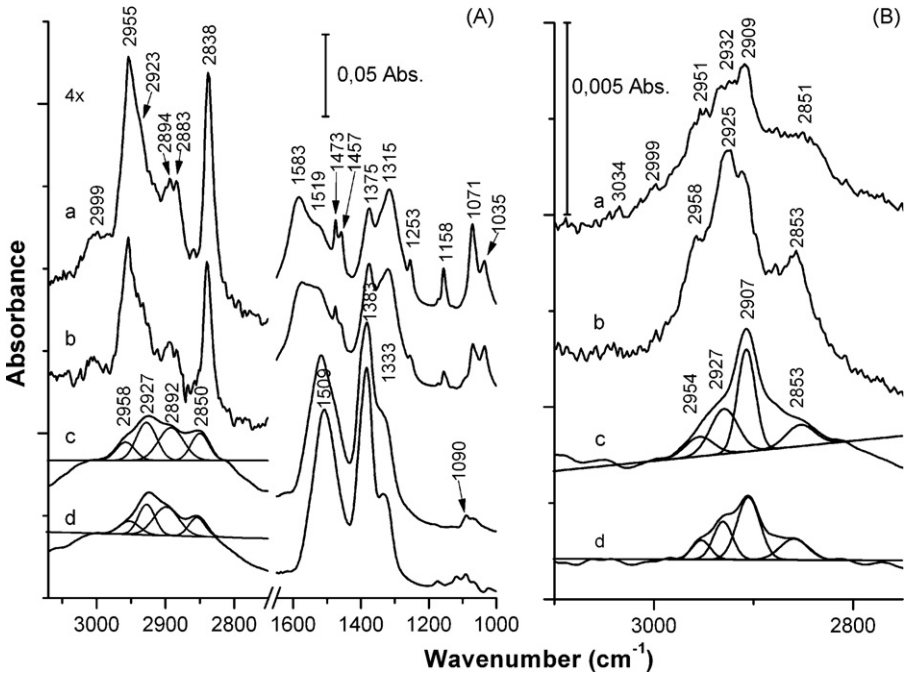

Fig. 1. FTIR spectra following the adsorption of DME on 1% Au/CeO_2 (A) and 1% Au/Al_2O_3 (B) at 300 K and after subsequent degassing at different temperatures. a, 300 K; b, 373 K; c, 423 K; d, 473 K.

~25% at 773 K. Note that pure CeO_2 reduced at 673 K exhibited a very little activity, even at 773 K we measured only less than 1% conversion. The situation was basically different on Al_2O_3-based catalysts. On 1% Au/Al_2O_3 the conversion of DME was about 80% at 723 K and the total conversion was reached at 773 K, but the production of hydrogen remained at low level in the whole temperature range (Fig. 3B). At lower temperature methanol was the main product. Above 673 K CH_4, CO, H_2 and CH_3OH were determined in decreasing quantities. The yield of H_2 did not exceed 20% even at 723–773 K. No deactivation of Au/Al_2O_3 was observed in 10 h at 773 K. Note that the pure Al_2O_3 also exhibited relatively high activity towards DME. The conversion was ~68% at 723 K and increased to ~88% at 773 K. The product distribution was practically the same as measured for Au/Al_2O_3, but less hydrogen was formed.

Taking into account the results obtained for different catalysts, an attempt was made to combine the advantageous catalytic properties of alumina- and ceria-supported Au. When 1% Au/CeO_2 and Al_2O_3 was separated by glass wool, the extent of the decomposition of DME was ~90% at 723 K and ~100% at 773 K. The selectivity for H_2 production scattered between 22 and 26% and the yield reached the value of 23% at 773 K. When 1% Au/CeO_2 was mechanically mixed with alumina the selectivity for H_2 above 600 K fell in the range of 30–35% and the yield for H_2 was 37% at 773 K. Higher values for H_2 production were obtained, when following the preparation method Au was deposited on Al_2O_3–CeO_2 mixed oxides. The selectivity value for H_2 was 35–40%, and the H_2 yield exceeded a value of 40% at 773 K. The product distribution is presented in Fig. 4A and B, whereas the values for the selectivity and yields of H_2 formation are plotted in Fig. 5A and B.

Adding water to DME (H_2O/DME = 1) exerted a dramatic influence on the product distribution. The amount of CH_4 and CO decreased and more hydrogen were produced (Fig. 4C and D). The selectivity for H_2 was almost 80%, while the yield for hydrogen formation approached the value of 73% (Fig. 5C and D). Following the reaction in time on stream at 773 K for 10 h we experienced no deactivation. When H_2O/DME ratio was increased to 3, only a slight further enhancement was measured, occurred in the values for hydrogen production.

In the study of the decomposition and reforming of ethanol [38] and DME [16] on Mo_2C/Norit catalysts we found that the presence of potassium markedly promoted the formation of hydrogen. We performed similar experiments in the present case. It appeared that the addition of 1% potassium to 1% Au/CeO_2–Al_2O_3 catalyst exerted

Table 1
Characteristic absorption bands of gaseous and adsorbed dimethyl ether and methanol on various solids.

Vibrational mode	DME(g) [34,35]	DME(a) Al_2O_3 at 150 K [35]	CH_3O(a) Al_2O_3 at 150 K [35]	CH_3O(a) CeO_2 at 523 K [36]	DME(a) CeO_2 at 300 K [17]	CH_3O(a) Rh/CeO_2 at 300 K [17]	DME(a) Au/CeO_2 at 300 K [present study]	DME(a) Au/SiO_2 at 373 K [present study]
$\nu_a(CH_3)$	2996 2925	2984 2922	2960	2911	2953	2948	2955	2958 2925
$\nu_s(CH_3)$ $2\delta(CH_3)$	2817 2887	2821 2890	2849	2803 2883	2841 2884	2838	2838 2889	2912 2859
$\delta(CH_3)$	1470 1456	1477 1459	1475 1420	1434	1436	1463	1473 1457	
$\gamma(CH_3)$	1244 1179	1252 1116	1081		1229 1159	1190	1253 1158	
$\nu_{as}(CO)$	1102	1092	1055	1108	1066	1095	1071	

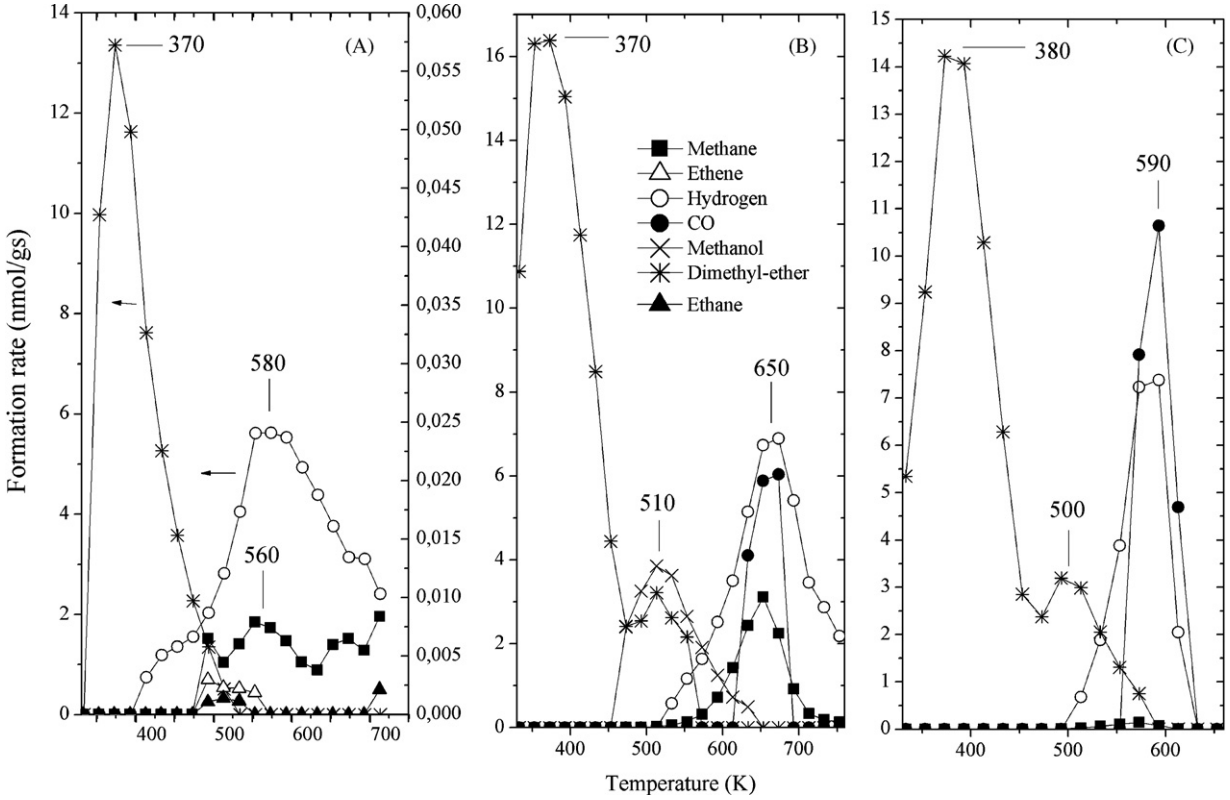

Fig. 2. TPD spectra following the adsorption of DME on 1% Au/CeO_2 (A), 1% Au/Al_2O_3 (B), and 1% $Au/CeO_2 + Al_2O_3$ (co-impregnated) (C) at 300 K.

a positive influence on the formation of hydrogen in the reforming of DME. In this case we measured the highest yield (86–87%) for hydrogen at 773 K. As shown in Fig. 6 this value remained unaltered in time on stream in the measured time, ~10 h.

3.5. TPR measurements

After completion of the catalytic experiments, TPR measurements were carried out (Fig. 7). The amount and the reactivity of the surface carbonaceous deposit depended on the reaction temperature. After the decomposition of DME on 1% $Au/CeO_2 + Al_2O_3$ catalysts at 773 K for 15 h, the surface carbon reacted with hydrogen only above 700 K, resulting in the formation of a large amount of methane ($T_p \approx 830$ K) and much less ethane and ethylene ($T_p = 705–730$ K) (Fig. 7A). After reforming of DME on the same catalyst under identical experimental conditions we identified the production of same compounds, but in much smaller quantities. The peak temperatures remained practically unaltered (Fig. 7B). This result suggests that the water prevents the deposition of carbonaceous species very likely reacting

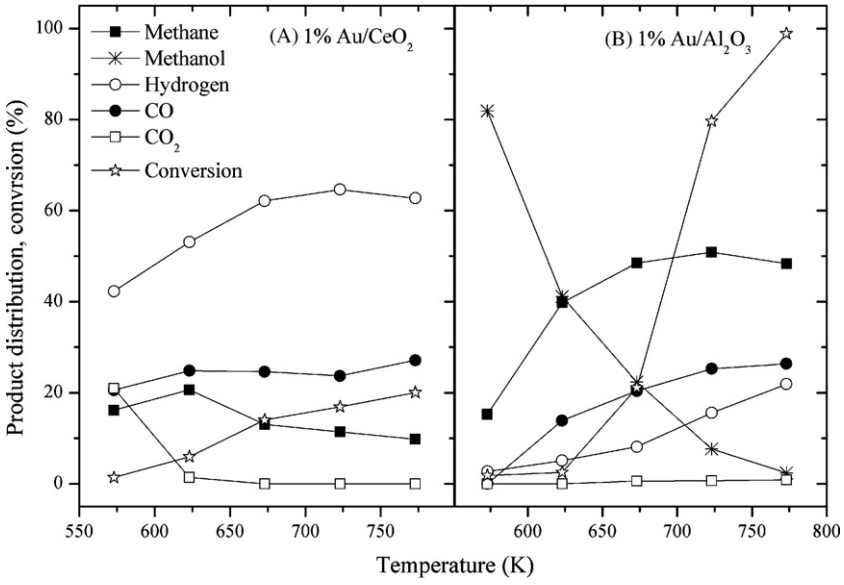

Fig. 3. Product distribution in the decomposition and reforming of DME on 1% Au/CeO_2 (A) and 1% Au/Al_2O_3 (B) at different temperatures.

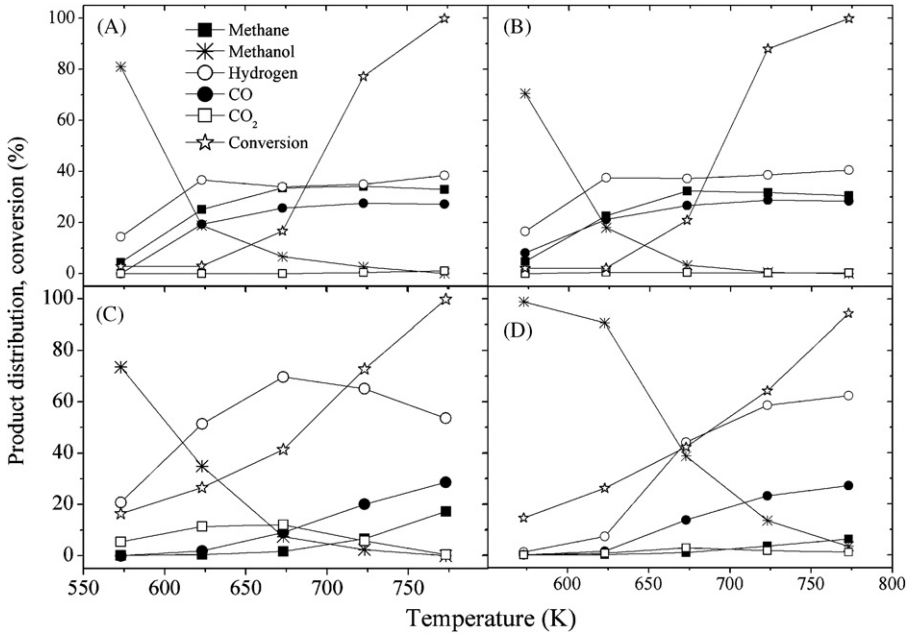

Fig. 4. Product distribution of the decomposition of DME on 1% Au/CeO_2 mixed with Al_2O_3 (A), 1% $Au/CeO_2 + Al_2O_3$ (co-impregnated) (B) and reforming of DME on 1% Au/CeO_2 mixed with Al_2O_3 (C), 1% $Au/CeO_2 + Al_2O_3$ (co-impregnated) (D).

with the surface species yielding the carbon-containing material.

4. Discussion

4.1. Interaction of DME with supported Au

The adsorption of DME with pure Au single crystal has not been studied, yet. In the case of Rh(1 1 1) we found that DME decreases the work function of the Rh maximum with 1.2 eV indicating that adsorbed DME has a positive outward dipole moment [37]. The vibrational modes of adsorbed DME on clean Rh(1 1 1) corresponded well to the gas-phase values. From the analysis of HREEL spectra of an annealed layer following DME adsorption at 100 K, spectral features indicative of the dissociation of adsorbed DME were not found. On an oxygen-dosed surface, however, methoxy species were clearly identified by HREEL spectroscopy [37].

We suppose that bulk Au should not be more reactive towards DME than the Rh. The situation is, however, could be different on gold nanoparticles, which may exhibit a much higher reactivity. However, it is not easy to prove this expectation as most of the oxidic supports can activate alone the adsorbed DME molecule. This is illustrated by the identical IR spectra for pure and Au-containing CeO_2. The situation is different on silica-supported Au as silica is inert towards DME. TPD and FTIR measurements revealed that DME adsorbs weakly and non-dissociatively on silica at 300 K: it desorbs with a $T_p = 373$ K. Following the adsorption of DME on 5% Au/SiO_2 at 300 K weak absorption bands can be identified at 2958 and 2853 cm^{-1} (Fig. 1B), which we attribute to the vibration of

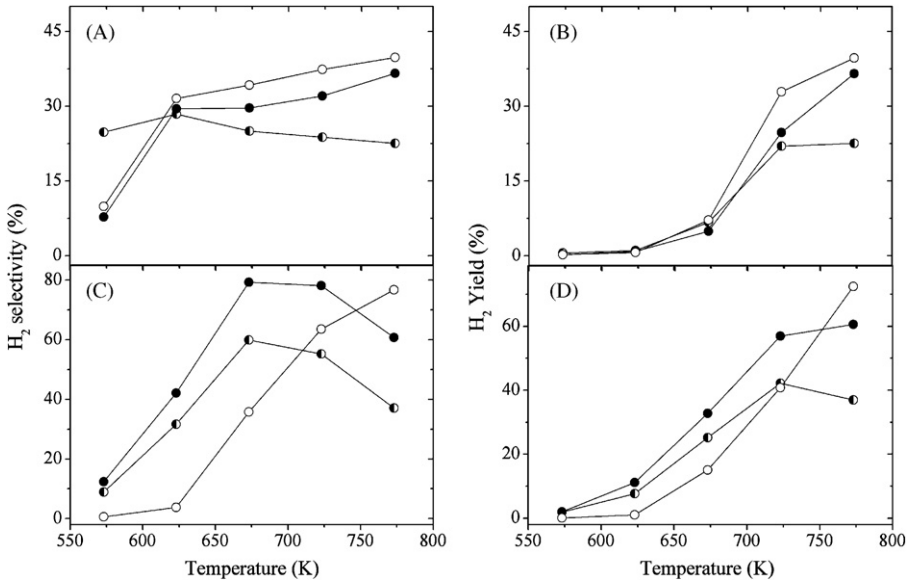

Fig. 5. The selectivity and yield of H_2 formation in the decomposition (A and B) and reforming of DME (C and D) on 1% $Au/CeO_2 + Al_2O_3$ catalyst. 1% Au/CeO_2 and Al_2O_3 is separated; (●) 1% Au/CeO_2 mixed with Al_2O_3; (○) 1% $Au/CeO_2 + Al_2O_3$ (co-impregnated).

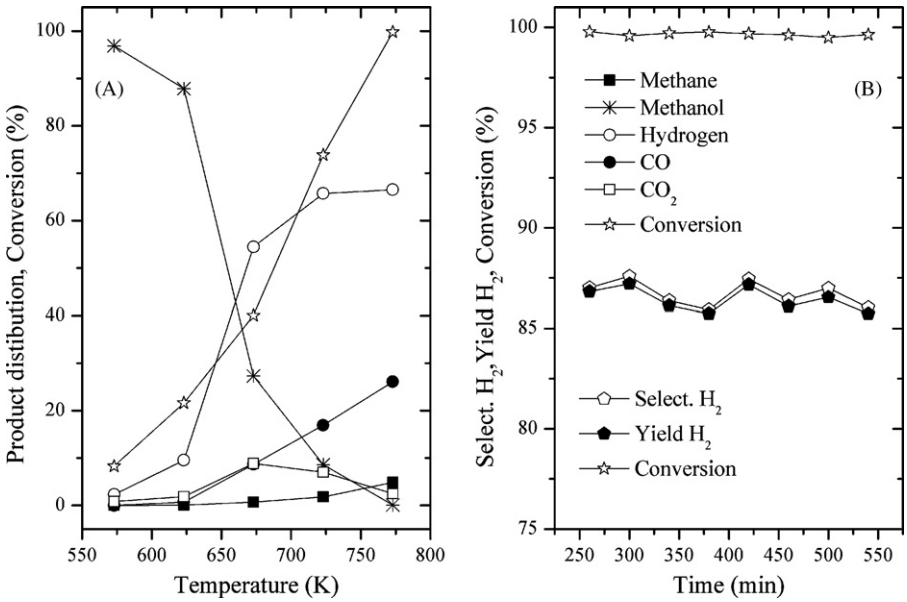

Fig. 6. Product distribution in the reforming of DME on 1% K + 1% $Au/CeO_2 + Al_2O_3$ (co-impregnated) catalyst at different temperatures (A). The selectivity and yield of H_2 formation in time on stream at 773 K (B).

methoxy species formed in the reaction

$$(CH_3)_2O_{(a)} = CH_3O_{(a)} + CH_{3(a)} \quad (1)$$

Accordingly, Au can promote the scission of one of the C–O bond in DME resulting in Au–OCH_3 surface complex. The vibration at 2925 cm^{-1} is very likely due to the ν_a of undissociated DME. This absorption band was observed in the IR spectrum of gaseous DME and also in that adsorbed DME on Al_2O_3 at 150 K [34,35]. The more intense absorption bands at around 2955, 2838, 2889, 1473, 1457, and 1071 cm^{-1} established on CeO_2-based samples are also due to methoxy species, very likely located on ceria. As there is no indication of the spectral feature determined for adsorbed CH_3 species [39,40], it is very likely that it is attached to the oxygen atom of CeO_2, also yielding a Ce–OCH_3 surface compound. The effect of gold in Au/CeO_2 is manifested in the lower stability of the above absorption bands, indicating the occurrence of the migration of adsorbed methoxy from the ceria onto the Au, and its faster decomposition on the metal. The development of the spectral features at 1583, 1375, and 1315 cm^{-1} are tentatively attributed to the formate formed in the reaction on ceria

$$OH_{(a)} + CO_{(a)} = HCOO_{(a)} \quad (2)$$

4.2. Reactions of DME

In our previous studies it was found that the decomposition and reforming of methanol and ethanol on supported Au nanoparticles sensitively depends on the nature of the supports [27,30]. Au/CeO_2 represented the most effective catalyst in both cases. The yield of hydrogen production from methanol reached the value of 93% at 773 K. As the C–C bond cleavage in the adsorbed ethanol occurs to only a limited extent even on Au/CeO_2, the production of H_2 from ethanol was much less. This feature appeared in the present case,

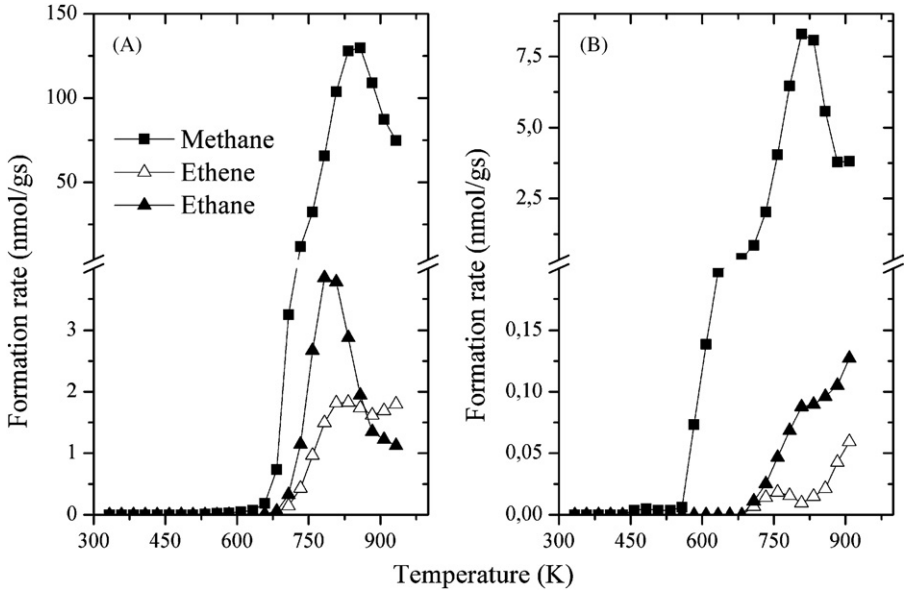

Fig. 7. TPR spectra for 1% $Au/CeO_2 + Al_2O_3$ (co-impregnated) after decomposition (A) and reforming (B) of DME at 773 K for 13 h.

when the rupture of C–C bond is probably the slowest step in the decomposition of DME Au/CeO_2: the conversion of DME remained relatively at low level, around 20% even at 773 K (Fig. 3A). Nevertheless, concerning the production of hydrogen, Au/CeO_2 exhibited the highest activity among the Au samples studied. In contrast, on Au/Al_2O_3, which catalyzed effectively the conversion of DME (Fig. 3B), the main reaction pathway was basically different. The primary product was methanol, which suggests the occurrence of the hydrolysis of DME with the participation of OH groups of alumina

$$CH_3–O–CH_{3(g)} + OH_{(a)} = 2CH_3OH_{(g)} \quad (3)$$

The use of $CeO_2 + Al_2O_3$ mixed oxide as a support for Au, however, resulted in the highest rate for the formation of hydrogen in both the decomposition and the reforming of DME (Figs. 4 and 5). This high activity can be attributed (i) to the hydration property of alumina, (ii) to the formation of methanol (Eq. (3)) and (iii) to the high reactivity of Au–CeO_2 interface in the activation and decomposition of methanol [27]

$$CH_3OH = CO + 2H_2 \quad (4)$$

In the explanation of high activity of Au/CeO_2 in the decomposition of methanol it was proposed that Au/CeO_2 contains a very reactive site [27]. This could be the interface between Au and partially reduced CeO_x, where an electronic interaction occurs between Au and the n-type CeO_2 semiconductor, similar to that discovered first between Ni and n-type TiO_2 [41]. Considering the rapid conversion of DME into methanol on the composite catalyst and the easy formation of methoxy species from methanol on solids studied, we assume that the slowest step in the generation of hydrogen from DME over $Au/CeO_2 + Al_2O_3$ catalyst is the cleavage of one of the C–H bonds in the methoxy species

$$CH_3O_{(a)} = CH_2O_{(a)} + H_{(a)} \quad (5)$$

Adding potassium to the $Au/CeO_2 + Al_2O_3$ catalyst further accelerated the formation of hydrogen in the reforming of DME, which can be probably attributed to the promoting effect of potassium on the water gas shift reaction

$$CO + H_2O = CO_2 + H_2 \quad (6)$$

which is well-catalyzed by CeO_2-supported metals and Mo_2C [38]. The fact that the methane content is also reduced on the K-dosed sample indicates that the rate of methane reforming

$$CH_4 + H_2O = CO + 3H_2 \quad (7)$$

is also enhanced on the promoted sample. We point out that potassium, by donating electrons to adsorbed H_2O and CO, can activate these molecules resulting in higher rates of their reaction [42].

5. Conclusions

(i) XPS studies demonstrated that Au nanoparticles reduced at 673 K contain Au^0 and a small amount of Au^+.
(ii) FTIR spectroscopy revealed the formation of methoxy species in the dissociation of DME on oxide-supported Au.
(iii) The direction of the decomposition of DME on Au catalysts depends on the nature of the support. Whereas Au/CeO_2 catalyses the production of hydrogen, on Au/Al_2O_3 the main process is the hydrolysis of DME. The combination of these properties and the use of $Au/CeO_2–Al_2O_3$ composite sample led to a very efficient catalyst for the production of hydrogen in both the decomposition and the reforming of DME.
(iv) The high activity is attributed to the easy formation of methanol from DME on alumina and to the high reactivity of Au–CeO_2 interface in the decomposition of methanol.
(v) Adding potassium to this catalyst promoted the production of hydrogen.

Acknowledgements

This work was supported by OTKA under contract number NI 69327 and K 81517.

References

[1] G. Sandstede, T.N. Veziroglu, C. Derive, J. Pottier (Eds.), Proceedings of the Ninth World Hydrogen Energy Conference, Paris, France, 1972, pp. 1745–1752.
[2] A. Haryanto, S. Fernando, N. Murali, S. Adhikari, Energy Fuels 19 (2005) 2098–2106.
[3] A.M. Rouhi, Chem. Eng. News 73 (1995) 37–39.
[4] J.-L. Li, X.-G. Zhang, T. Inui, Appl. Catal. A: Gen. 147 (1996) 23–33.
[5] T. Fleish, Stud. Surf. Sci. Catal. 107 (1997) 117–125.
[6] G.A. Olah, Á. Molnár, Hydrocarbon Chemistry, Wiley, New York, 2003, and references therein.
[7] A. Kecskeméti, R. Barthos, F. Solymosi, J. Catal. 258 (2008) 111; A. Széchenyi, F. Solymosi, Catal. Lett. 127 (2009) 13–19.
[8] V.V. Galvita, G.L. Semin, V.D. Belyaev, T.M. Yurieva, V.A. Sobyanin, Appl. Catal. A: Gen. 216 (2001) 85–90.
[9] K. Takeishi, H. Suzuki, Appl. Catal. A: Gen. 260 (2004) 111–117.
[10] T. Nishiguchi, K. Oka, T. Matsumoto, H. Kanai, K. Utani, S. Imamura, Appl. Catal. A: Gen. 301 (2004) 66–74.
[11] K. Faungnawakij, Y. Tanaka, N. Shimoda, T. Fukunaga, S. Kawashima, R. Kikuchi, K. Eguchi, Appl. Catal. A: Gen. 304 (2006) 40–48.
[12] T. Kawabata, H. Matsuoka, T. Shishido, D. Li, Y. Tian, T. Sano, K. Takehira, Appl. Catal. A: Gen. 308 (2006) 82–90.
[13] T.A. Semelsberger, K.C. Ott, R.L. Borup, H.L. Greene, Appl. Catal. B: Environ. 61 (2005) 281–287; T.A. Semelsberger, K.C. Ott, R.L. Borup, H.L. Greene, Appl. Catal. B: Environ. 65 (2005) 291–300.
[14] N. Laosiripojana, S. Assabumrungrat, Appl. Catal. A: Gen. 320 (2007) 105–113.
[15] T. Fukunaga, N. Ryomon, S. Shimazo, Appl. Catal. A: Gen. 348 (2008) 193–200, and references therein.
[16] F. Solymosi, R. Barthos, A. Kecskeméti, Appl. Catal. A: Gen. 350 (2008) 30–37.
[17] G. Halasi, T. Bánsági, F. Solymosi, ChemCatChem 1 (2009) 311–317.
[18] K. Faungnawakij, N. Shimoda, T. Fukunaga, R. Kikuchi, K. Eguchi, Appl. Catal. B: Environ. 92 (2009) 341–350, and references therein.
[19] M. Haruta, T. Kobayashi, H. Sano, N. Yamada, Chem. Lett. 2 (1978) 405–408.
[20] A. Stephen, A.S.K. Hashmi, G.J. Hutchings, Angew. Chem. Int. Ed. 45 (2006) 7896–7936.
[21] J.G. Hardy, M.W. Roberts, Chem. Commun. (1971) 494–495; M.W. Roberts, T.I. Stewart, in: P. Hepple (Ed.), Proc. of Chemisorption and Catalysis, Institute of Petroleum, 1970.
[22] M. Haruta, A. Ueda, S. Tsubota, R.M. Torres Sanchez, Catal. Today 29 (1996) 443–447.
[23] F. Boccuzzi, A. Chiorino, M. Manzoli, J. Power Sources 118 (2003) 304–310.
[24] M. Manzoli, A. Chiorino, F. Boccuzzi, Appl. Catal. B: Environ. 57 (2005) 201–209.
[25] A. Nuhu, J. Soares, M. Gonzalez-Herrera, A. Watts, G. Hussein, M. Bowker, Top. Catal. 44 (2007) 293–297.
[26] I. Mitov, D. Klissurski, C. Minchev, Comptes. Rendus. De L. Acad. Bulgare Des Sci. 61 (2008) 1003–1006.
[27] A. Gazsi, T. Bánsági, F. Solymosi, Catal. Lett. 131 (2009) 33–41.
[28] R. Perez-Hernández, A. Gutierrez-Martinez, C.E. Gutierez-Wing, Int. J. Hydrogen Energy 32 (2007) 2888–2894.
[29] P.-Y. Sheng, G.A. Bowmaker, H. Idriss, Appl. Catal. A: Gen. 261 (2004) 171–181.
[30] A. Gazsi, T. Bánsági, F. Solymosi, Catal. Today, in press.
[31] P. Burroughs, A. Hamnett, A.F. Orchard, G. Thornton, J. Chem. Soc. Dalton Trans. (1976) 1686–1698.
[32] E.D. Park, J.S. Lee, J. Catal. 186 (1999) 1–11.
[33] A. Karpenko, R. Leppelt, V. Plzak, R.J. Behm, J. Catal. 252 (2007) 231–242.
[34] T.P. Bebe Jr., J.E. Crowell, J.T. Yates Jr., J. Phys. Chem. 92 (1988) 1296–1301.
[35] J.G. Chen, P. Basu, T.H. Ballinger, J.T. Yates Jr., Langmuir 5 (1989) 352–356.
[36] A. Badri, C. Binet, J.C. Lavalley, G. Blanchard, J. Chem. Soc. Faraday Trans. 93 (1997) 1159–1168.
[37] L. Bugyi, F. Solymosi, Surf. Sci. 385 (1997) 365–375.
[38] A. Koós, R. Barthos, F. Solymosi, J. Phys. Chem. C 112 (2008) 2607–2612.
[39] F. Solymosi, G. Klivényi, J. Electr. Spectr. 64/65 (1993) 499–506.
[40] J. Raskó, F. Solymosi, Catal. Lett. 54 (1998) 49–54.
[41] F. Solymosi, Catal. Rev. 1 (1967) 233–255.
[42] M.P. Kiskinova, Stud. Surf. Sci. Catal. 70 (1991) 1–345.